Measuring infrasound outdoors with a focus on wind turbines: the benefits of a wind-shielding dome

Sarah D'Amico[a,*], Timothy Van Renterghem[a], Dick Botteldooren[a]

[a]*Ghent University, Department of Information Technology, WAVES Research Group, Technologiepark 126, B 9052 Gent-Zwijnaarde, Belgium*

[*] Author to whom correspondence should be addressed. Electronic mail: Sarah.DAmico@UGent.be

Keywords: wind-induced noise; wind turbine noise; infrasound; aeroacoustics; measurement methodologies.

Wind-induced microphone noise complicates infrasound measurements considerably. A wind-shielding dome for signal-to-noise ratio improvement of acoustic pressure infrasound frequencies was designed and tested. The semi-spherical shape aimed at maximizing the pressure averaging of large atmospheric turbulent eddies while keeping the structure reasonably compact. The insertion loss of the dome was measured in a semi-anechoic chamber (in absence of flow) and showed nearly full transparency in the low frequency range. In an outdoor test, wind turbine infrasound was simultaneously measured with an uncovered and a dome-covered low-frequency microphone under different wind speeds and turbulence intensities. Largest improvements of the signal-to-noise ratio were measured at high mean wind speeds for frequencies down to 0.5 Hz. The dome allowed to clearly identify the infrasonic tonal components of wind turbines that were otherwise completely covered by the wind-induced microphone noise even at low mean wind speeds. The use of the dome thus opens possibilities for more accurately measuring infrasonic immissions from e.g. wind turbines.

1. Introduction

Wind-induced microphone noise is a common concern in outdoor environmental noise assessment and a relevant source of infrasound. The intrinsic turbulent eddies in the air flow produce low-frequency pressure fluctuations [1]. Especially when interacting with objects such as microphones, sound sources appear with a non-negligible power [2]. A problem thus arises when measuring wind turbine infrasound as it always co-occurs with wind-induced microphone noise in this frequency range. Distinguishing between the two noise sources is arduous and the signal-to-noise ratio (SNR) is often poor.

The use of foam wind screens is a consolidated practice to reduce wind-induced microphone noise. Notwithstanding their practical importance, their physics is still not completely clarified. Strasberg [3] developed an analytical model relating the power spectral density (PSD) for wind screen noise to the mean wind speed. His model was well validated for a large set of measurements but limited to low turbulence flow, neglecting atmospheric (inflow) turbulence noise [1].

The predominance of atmospheric turbulence in generating wind-induced microphone noise is confirmed by van den Berg [4]. In particular, for a characteristic-length ratio much smaller than 0.3, wind-induced microphone noise is entirely attributed to inflow turbulence, while for a characteristic-length ratio larger than 0.3, the wind screen acts as a first-order low pass filter for turbulence fluctuations. The characteristic-length ratio is defined as the ratio between the characteristic-length of the wind screen (L_s) and the characteristic-length of the turbulence eddies ($U_c \,/\, f$) where U_c is the convective velocity ($U_c \sim 0.7U$, with U being the mean wind speed) and f the frequency. For a spherical wind screen, L_s is the diameter of the screen.

The use of ground-positioned microphones and (double) wind-screens are common practice nowadays to measure the noise immission of wind turbines. Although wind-induced microphone

noise can be significantly decreased in the high and middle frequency range in this way, the SNR remains inadequate at low and infrasound frequencies; reductions of wind-induced microphone noise are only a few decibels [5], [6]. A main problem is that the efficiency of a wind screen at low and infrasound frequencies is limited by its dimension and thus remains unable to shield the noise production of large turbulent eddies.

Large wind fences have been investigated to reduce wind-induced infrasound at microphones. These are devices commonly used e.g. in agricultural application to reduce wind velocity to protect cultivations. The applications of large wind fences in environmental noise assessment has been analyzed by several researchers. Hedlin et al. [7] tested the behavior of a large circular wind barrier opened at the top. A 2 m high and 5.5 m large fence of 50 % porosity was tested under different wind speeds. Pressure fluctuations inside and outside the barrier were monitored. Abbott et al. [2] analyzed wind fences of different porosities. In the studies of Hedlin et al. and Abbott et al. [2],[7], reductions of mean wind speed inside the fence resulted in proportional reductions of wind-induced microphone noise at mid and low frequencies, while this was not the case at infrasonic frequencies. For a characteristic-length ratio below 1 the wind-induced microphone noise reductions dropped drastically [2], [7]. Large wind fences were shown to be inefficient in reducing wind-induced microphone noise for eddies larger than their characteristic dimension. However, modern large wind turbines generate infrasound tonal frequencies down to 0.8 Hz linked to the blade passing frequency [8] on top of broadband infrasound (so-called inflow turbulence noise). In order to provide sufficient wind-induced microphone noise reduction to obtain a satisfactory SNR for assessment of infrasound from wind turbines, much larger wind fences would be needed, making them highly impractical.

Hedlin et al. discussed the inefficiency of large open wind fences at low and infrasonic frequencies [7], and expected that a spherical wind barrier could be a more effective and compact device for infrasonic wind-induced microphone noise reduction. This idea of porous domes was then investigated by Noble et al. [9] for military applications, showing promising reductions of wind-induced microphone infrasound. Abbott et al. [10] and Raspet et al. [11] proposed a semi-empirical model for wind-induced microphone noise reductions for open fences and domes. Their model identified three regions of interest: the unperturbed region, which predominates only in the frequency range where the screen in not effective (lowest frequencies); the surface region and the region inside the enclosure. The surface contribution resulted to be predominant [11], [12] for wind-induced microphone noise reductions. Raspet et al. [11] hypothesized that the lower limit of the frequency range at which a hemispherical-dome is effective is given by a characteristic-length ratio of approximately 0.4 [11].

The current paper investigates a semi-spherical dome fence as a compact and efficient device to improve the SNR for infrasound measurements in general, but with a clear focus on wind turbine noise monitoring. In this work, a suitable geometry and textile porosity were sought based on existing literature. The acoustic insertion loss of the dome in absence of wind was tested in a laboratory environment. Its performance was then validated outdoors while measuring infrasonic wind turbine tonal components under different wind speeds and turbulence intensities in a long-term field test.

2. Dome design

A vertical impervious barrier in a wind flow generates a flow perturbation. The air flow encounters a stagnation point in front of the barrier, will accelerate near the top and faces an adverse pressure gradient behind it, leading to flow separation. Making the barrier porous allows

part of the flow to pass through. In this way, the stagnation point in front of the barrier is eliminated and the adverse pressure gradient behind the barrier is reduced. The porous barrier not only reduces the mean wind speed, but also affects the outer flow and the turbulence generation. Due to the vertical shape, however, flow acceleration is still to be expected at the top of the barrier and an adverse pressure gradient behind the porous fence will still appear.

Applying a more aerodynamic geometry to the structure of the fence was thought to further improve its effect on the flow passing around the barrier. In particular, this would supplementary reduce the adverse pressure gradient behind the barrier influencing the turbulence interactions around it. The goal is to enhance wind-induced noise reductions for turbulence structures down to $f \cdot L_d/U_c$ between 0.3 and 0.4, in accordance with the theories on spherical wind screens [4] and porous domes [11]. In order to be effective at low frequencies and infrasound and for U from 2 to at least 8 m/s, a characteristic length of approximately 2 m would be needed. For the dome acting as a wind shield, the height of the dome was chosen as the characteristic length (L_d), in accordance with the scientific literature on wind barriers [7]. For practical reasons, a commercially available dome-shaped PVC structure of 2.20 m height and 2.60 m base diameter was used.

The dome was covered with a commercially available thin wind breaking textile with square openings. The porosity of such a textile is a crucial design parameter in minimizing the pressure fluctuations at the microphone [10].

Inside such an enclosure, the pressure fluctuations at a microphone are caused by the direct interaction between the microphone and the local flow [1], [10] and the pressure fluctuations at the surface of the fence [10]. The former is significantly reduced by a screen enclosure [12] and the latter is a contribution added by the presence of the dome [11]. The combined effect of these contributions was found to be minimum for enclosures of middle porosities [2], [9], [11] yielding

the largest wind-induced microphone noise reductions. Based on this existing literature and available [13] textiles porosities, a porosity (defined as the ratio between the sum of the surfaces of all the individual openings and its total area) of 35.7 % was chosen.

3. Dome testing

3.1. Acoustical insertion loss in absence of wind

The sound transmission of the dome was tested in a semi-anechoic chamber. The signal at the uncovered microphone was compared with the one at the dome-covered microphone and their differences were calculated at the detail of 1/3rd octave bands. The test location was a semi-anechoic chamber of 5x9 m^2 at Ghent University. The B&K PULSE analysis software platform was used to perform the measurements with a GRAS 46 AZ low-frequency microphone capsule. An ICP amplifier of PCB was used to condition the microphone signal. The PULSE system was also used to generate a pink noise source signal and the test was performed using a subwoofer with a frequency range from 20 to 175 Hz. The microphone was calibrated at 1 kHz with a 94 dB Svantek 30 A Class 1 acoustic calibrator. Afterwards, the response of the microphone was also evaluated at 250 Hz with a B&K Pistonphone calibrator. The test set up is illustrated in Fig. 1. Two microphone positions were considered: one on the ground (configuration 1) and the other one on a tripod (configuration 2), both placed at the center of the dome. The two different heights were considered to evaluate the attenuation of the dome on the height of the microphone. The subwoofer was positioned so that the angles of the incident acoustic waves at the microphones are comparable to the ones that can be experienced when measuring noise immissions from wind turbines.

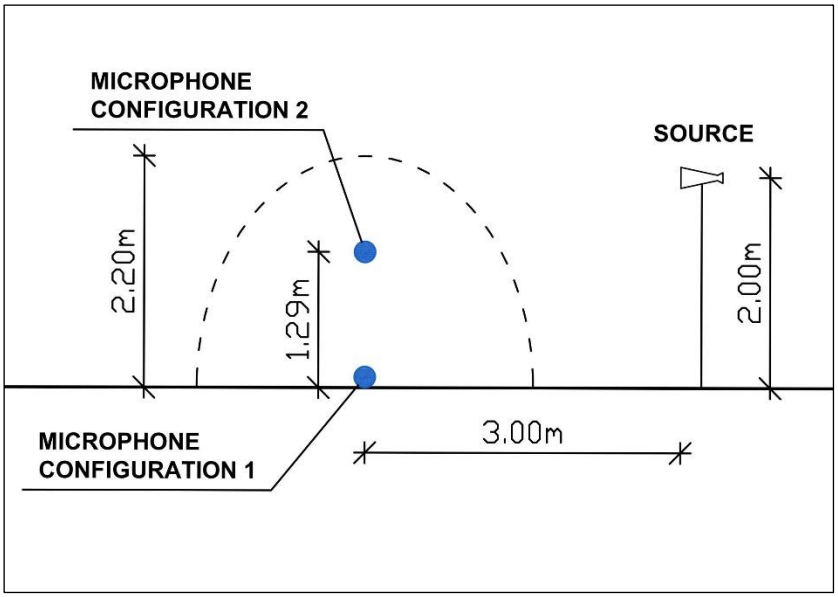

Fig. 1. Acoustic transparency test setup in the semi-anechoic room in absence of wind.

Measurements with the uncovered microphone were first performed; secondly the dome was mounted and placed around the microphone and measured in an identical way. For practical reasons, it was necessary to move the microphone while changing the measurement setup. As the floor of the chamber is rigid, the positioning of microphone can have an effect on the measurements as pronounced interferences might appear. Therefore, the repositioning error has been assessed. For each of the 4 repetitions, the microphone was moved out and back to its intended testing position. In case the dome was present, the dome was also slightly twisted around its center each time. The measurements were also acquired 10 minutes apart from each other to validate the temporal stability of the loudspeaker since measurements were not performed simultaneously. Fig. 2 illustrates the differences in decibels (so called insertion loss) between the uncovered and the dome-covered microphone for the two microphone positions for the 1/3rd octave bands from 20 to 200 Hz.

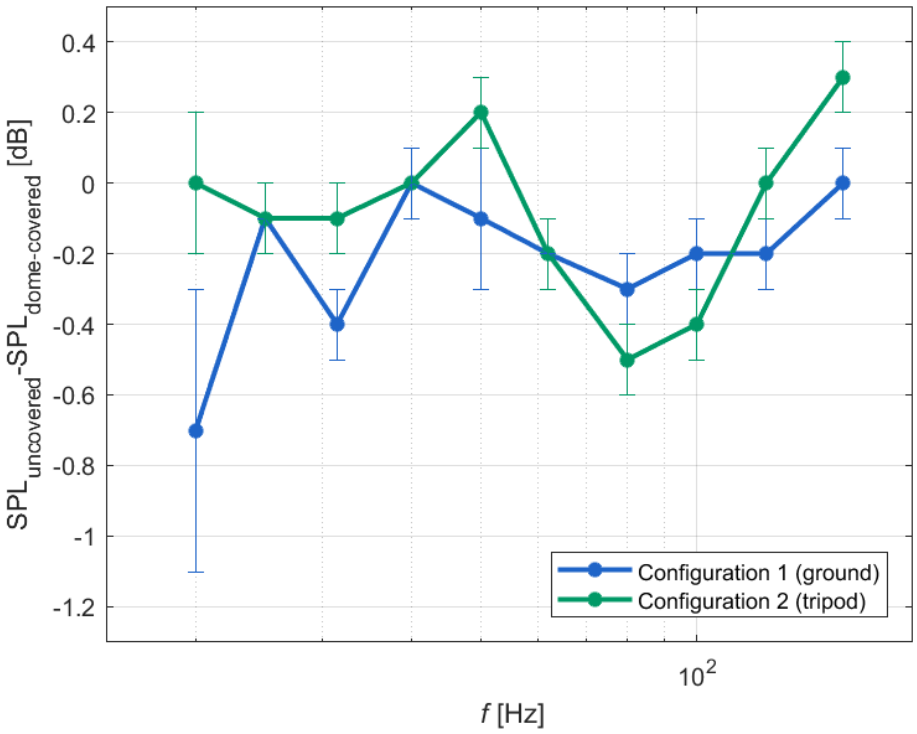

Fig. 2. Acoustic transparency test results, showing the difference in sound pressure level between the uncovered and dome-covered microphone. The error bars have a total length of two times the standard deviation as a result of repositioning the microphones and/or turning of the dome.

The insertion losses of the dome show to be smaller than 0.5 dB for 1/3rd octave bands with central frequencies from 20 to 200 Hz. Level differences smaller than 0.1 dB are seen for frequencies below 50 Hz. Some amplification by the dome can be observed but not exceeding 0.7 dB. A larger standard deviation is found at 20 Hz for the ground microphone, probably by variations in external sound and vibrations still entering the semi-anechoic room. Although there are some difficulties in exactly measuring the insertion loss of the dome, it can be concluded that the wind-shielding dome is nearly acoustically transparent in the low frequency range. Due to the limitations of the subwoofer and of the semi-anechoic chamber, measurements could not be

performed at lower frequencies. However, the near-acoustic transparency achieved down to 20 Hz makes it highly unlikely that this would not be the case at even lower frequencies.

3.2. Field test

3.2.1. Location and instrumentation

The performances of the dome in improving the SNR for wind turbine infrasound measurements were tested at the Melle Wind Farm on the terrain of Ghent University. The sound pressure levels immissions were measured simultaneously by an uncovered and a dome-covered microphone in a long-term measurement campaign.

The wind farm at the measurement location is composed of three Enercon E28 of 2 MW each, deployed at a distance of approximately 450 m from each other in the NW-SE direction as illustrated in the Google Earth image in Figure 3. The three wind turbines are three-bladed, pitch-controlled wind turbines with hub height of 108 m and 82 m rotor diameter. The wind turbines reach the rated power at 12.5 m/s mean wind speed and have a cut-in wind speed of 2 m/s.

Fig. 3. Aerial photographs of the outdoor test site. The measurement location is indicated by the red marker.

The surrounding environment is characterized by fully flat agricultural terrain with some sparse buildings located at a distance of 200 m from the microphones and a main motorway at approximately 250 m.

Two GRAS 46 AZ low frequency microphones and preamplifiers were used together with two Alix System single board computers for continuous recordings at a sampling frequency of 48 kHz. The internal filtering of the soundcard of the Alix system was flattened in the infrasonic frequency range. Microphones were equipped with rain protections and 10-centimenter diameter wind screens and the equipment was powered by direct power connection. The Svantek 30 A Class 1 acoustic calibrator was used to calibrate the microphones at 1 kHz and 94 dB; recording the calibration signal was repeated on a weekly basis. A Gill 3D sonic anemometer with 20 Hz acquisition frequency was used to monitor wind conditions. Precipitation data was acquired by the weather station of the Royal Meteorological Institute of Belgium located at about 8 m from the microphones. The operational data of the wind turbines were also available.

The two microphones were placed at a distance of 30 m from each other and at a height of 0.5 m above ground. The 3D sonic anemometer was placed in the proximity of the microphones at 10 m height. The measurements were deployed from September to December 2019 and from April to May 2020. Fig. 4 shows the schematics of the set up while Fig. 5 shows some photographs.

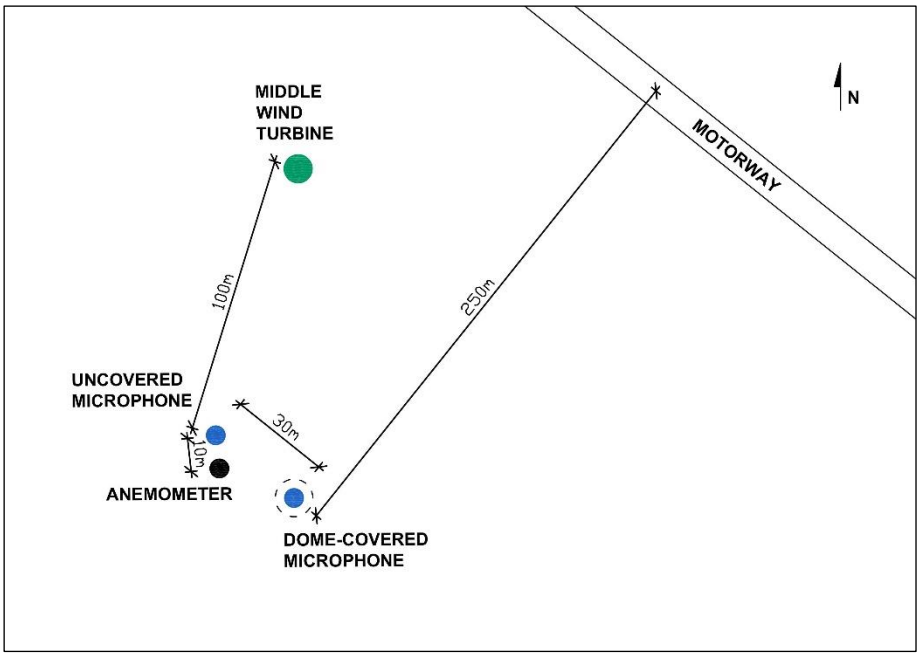

Fig. 4. Schematics of the field measurement set up.

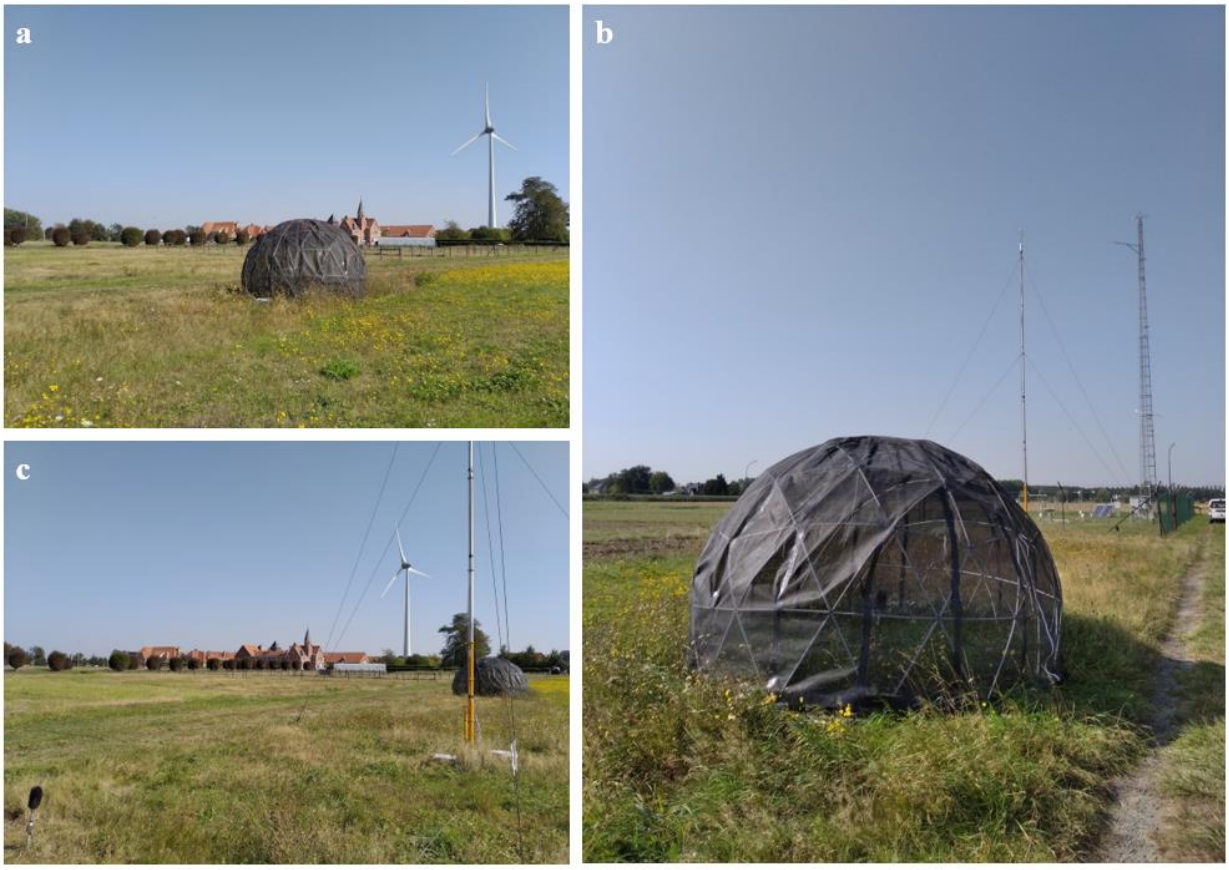

Fig. 5. Field measurement set up.

Data from rainy days were excluded from the measurements. Recordings with clearly identified close-by noise sources were removed as well upon listening during the periods when the use of agricultural machines in the proximity of the microphones were reported. The recordings were analyzed as one-minute samples, and averaged to ten-minute power spectral density (PSD) spectra from both microphones. PSD differences from the two microphones were also calculated on a 10-minute base.

The wind speed and the wind direction were acquired at a frequency of 20 Hz. The wind speed data were averaged for 10-minute intervals calculating the resulting mean wind speed and turbulence intensity. The wind direction data were assigned to sectors of 30° and the dominant sector in each 10-minutes interval was assessed. The ten-minute PSD spectra and spectral differences at both receivers were sorted for wind sector, mean wind speed and turbulence intensity.

For each group, PSD spectra and PSD spectra differences were averaged linearly for both microphones. Only atmospheric conditions with a minimum of 8 hours of continuous recordings were retained. This corresponds to 480 one-minute basic spectra, averaged to 48 ten-minute averaged data.

3.2.2. Field test results and analysis

Figures from 6 to 10 illustrate the absolute PSD levels from the uncovered and the dome-covered microphone for different wind conditions and for all the wind directions when all three wind turbines where operating. The measurements are presented in function of both the sound frequency and the characteristic-length ratio.

Fig. 6 presents the absolute measured levels for mean wind speeds from 2 to 7 m/s. Figures from 7 to 10 illustrate the values for 2, 3, 5 and 6 m/s mean wind speed, respectively, for different turbulence intensity (TI) conditions.

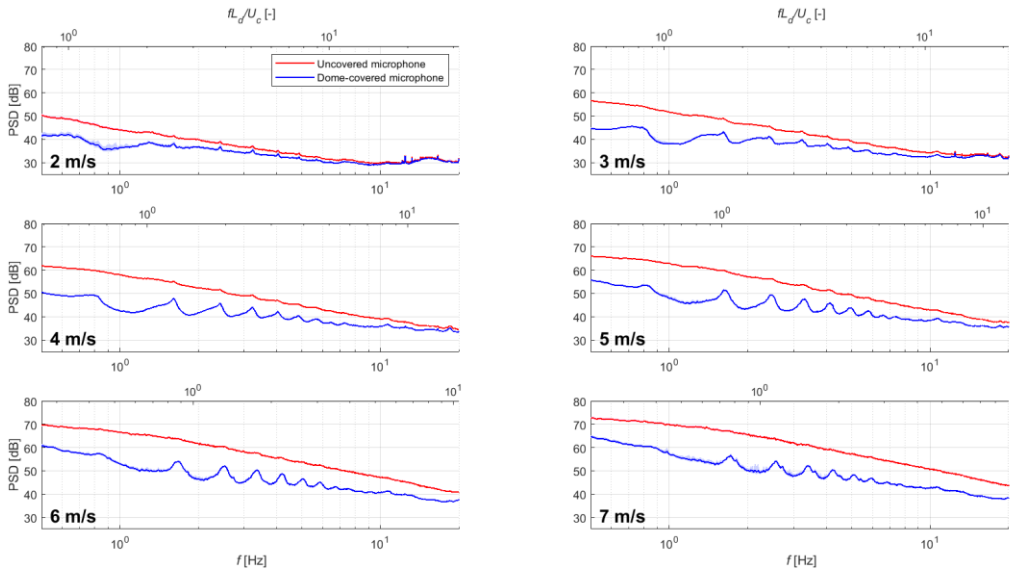

Fig. 6. (Absolute) PSD spectra for the uncovered and dome-covered receiver for 2, 3, 4, 5, 6 and 7 m/s mean wind speeds in function of sound frequency (lower horizontal axis) and characteristic-length ratio (upper horizontal axis). The 95 % confidence intervals are calculated with the bootstrapping method, assuming no specific statistical distribution of the data, and are depicted as shaded areas.

For all the cases presented in Fig. 6 the acoustic signature of the wind turbine is visible at the dome-covered microphone, showing clear peaks at the harmonics of the blade passing frequency (BPF). In contrast, at the uncovered microphone, these tonal components are almost completely (untill 5 m/s) or completely (from 6 m/s on) submersed in infrasonic wind induced microphone noise.

For the 2 m/s mean wind speed, the levels measured at the dome-covered and non-dome covered microphone coincide for frequencies above 5 Hz. Below 5 Hz, the measurements start to

diverge reaching a 10-decibel difference below 0.8 Hz. As the mean wind speed increases, both the values inside and outside the dome increase. At the same time, also their differences increase indicating a stronger contribution of the wind-induced microphone noise at the uncovered microphone than at the dome-covered microphone.

The BPF itself can be seen in most measurements. From the operational data of the wind turbines, it is expected to appear between 0.5 Hz (at 2 m/s mean wind speed) and 0.8 Hz (at 7 m/s mean wind speed). The BPF, even with the dome-covered microphone, is still partly masked by either wind turbine inflow noise or wind-induced microphone noise not completely removed at these extremely low frequencies. The BPF is most visible at 4 m/s and 5 m/s.

The behavior of the absolute PSDs are further analyzed for different TIs. For 2 and 3 m/s (Fig. 7 and 8), six TI conditions are compared. For the lowest TI condition of 10 %, levels from the uncovered and the dome-covered microphone are approximately the same along the full frequency range. The signatures of the wind turbines are visible from both microphones at 10 % TI and 2 and 3 m/s mean wind speed.

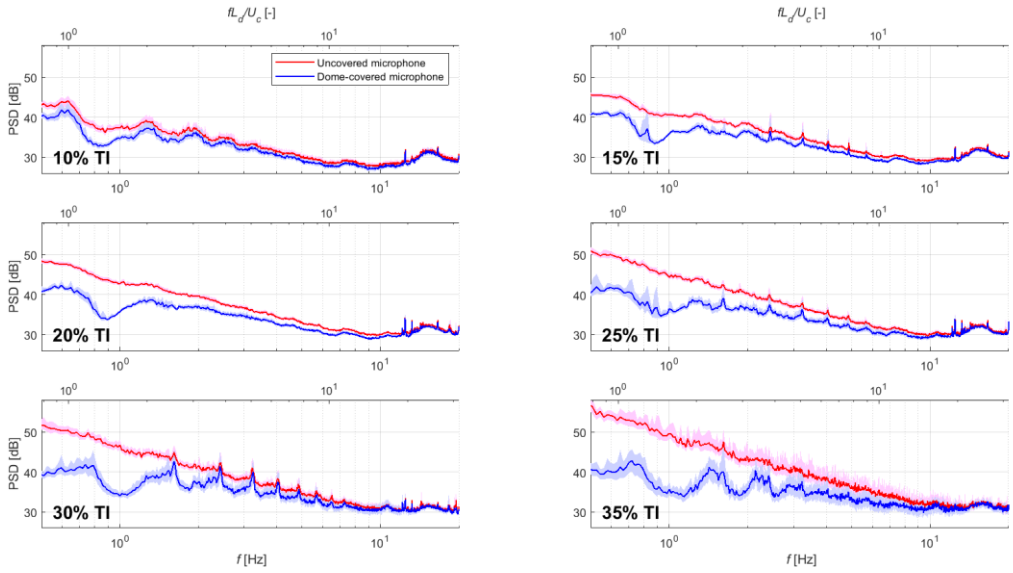

Fig. 7. (Absolute) PSD spectra for the uncovered and dome-covered microphone for 2 m/s mean wind speed and 10, 15, 20, 25, 30 and 35% turbulence intensity in function of sound frequency (lower horizontal axis) and characteristic-length ratio (upper horizontal axis). The 95 % confidence intervals are calculated with the bootstrapping method, assuming no specific statistical distribution of the data, and are depicted as shaded areas.

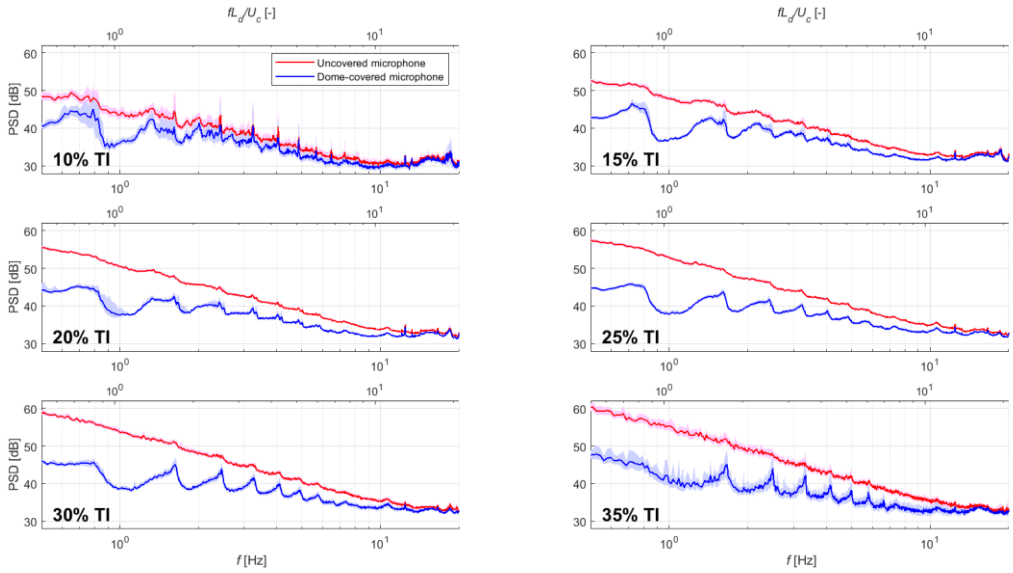

Fig. 8. (Absolute) PSD spectra for the uncovered and dome-covered microphone for 3 m/s mean wind speed and 10, 15, 20, 25, 30 and 35% turbulence intensity in function of sound frequency (lower horizontal axis) and characteristic-length ratio (upper horizontal axis). The 95 % confidence intervals are calculated with the bootstrapping method, assuming no specific statistical distribution of the data, and are depicted as shaded areas.

When the TI increases, the PSD levels inside the dome do not increase significantly and the overall level stays stable. At 0.5 Hz, levels at the dome-covered microphone remain at about 40 dB for all TIs at 2 m/s mean wind speed and at 45 dB for all TIs at 3 m/s mean wind speed. The values of the uncovered microphone vary much stronger with TI. At 0.5 Hz, the level at the

uncovered microphone increases with 10 dB from 10 to 30 % TI, both at 2 and 3 m/s mean wind speed.

The levels from the uncovered microphone already contain a lot of wind-induced microphone noise starting at 15 % TI. Although still present, the peaks due to the BPF and its harmonics are covered and difficult to visualize. For 3 m/s mean wind speed and TI above 25 % the signature becomes almost undetectable. For all the TI cases, the levels inside the dome present sharp peaks. Comparison between the two results thus indicates a significant improved SNR due to the presence of the dome at infrasonic frequencies.

The current data nicely shows that also for low mean wind speeds, wind-induced infrasonic microphone noise can be high, hindering tonal detection. Furthermore, the limited dependency of the PSDs inside the dome on the turbulence intensity indicates that the effect of the dome is related to the interaction with the turbulence structures more than to the mean wind speed reduction.

Similar trends can be observed for higher mean wind speeds where the improvement in SNR becomes even more evident. For 5 and 6 m/s mean wind speed (Fig. 8 and 10) at the uncovered microphone measurement, it is not possible to identify the wind turbines. In contrast, they can be clearly seen at the dome-covered microphone for all the TI cases. For 6 m/s mean wind speed, the maximum wind-induced microphone noise reduction is found between characteristic-length ratio 0.4 and 0.6 .

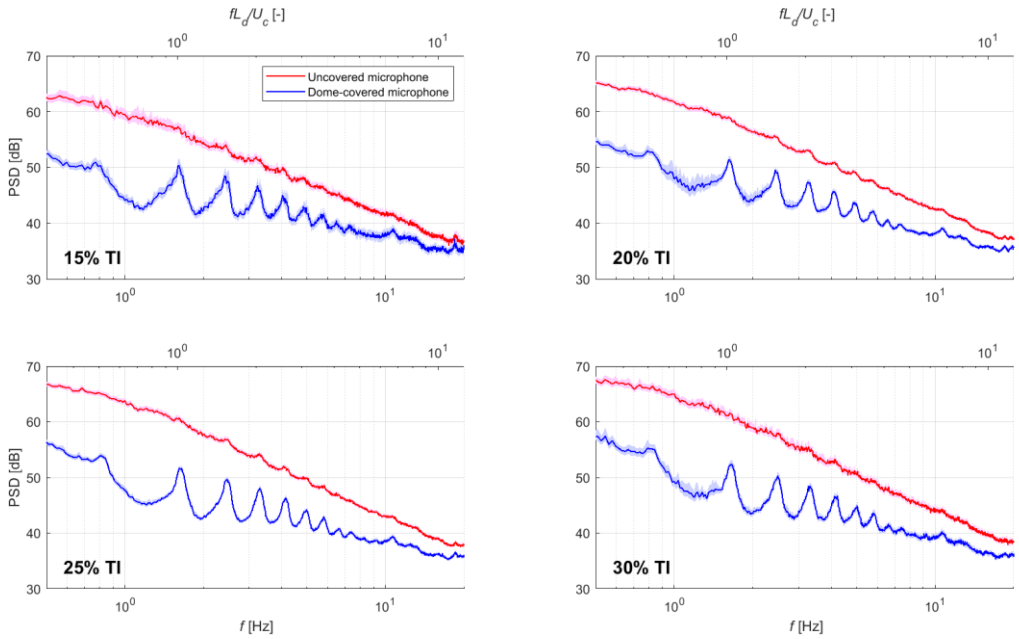

Fig. 9. (Absolute) PSD spectra for the uncovered and dome-covered microphone for 5 m/s mean wind speed and 15, 20, 25 and 30 % turbulence intensity in function of sound frequency (lower horizontal axis) and characteristic-length ratio (upper horizontal axis). The 95 % confidence intervals are calculated with the bootstrapping method, assuming no specific statistical distribution of the data, and are depicted as shaded areas.

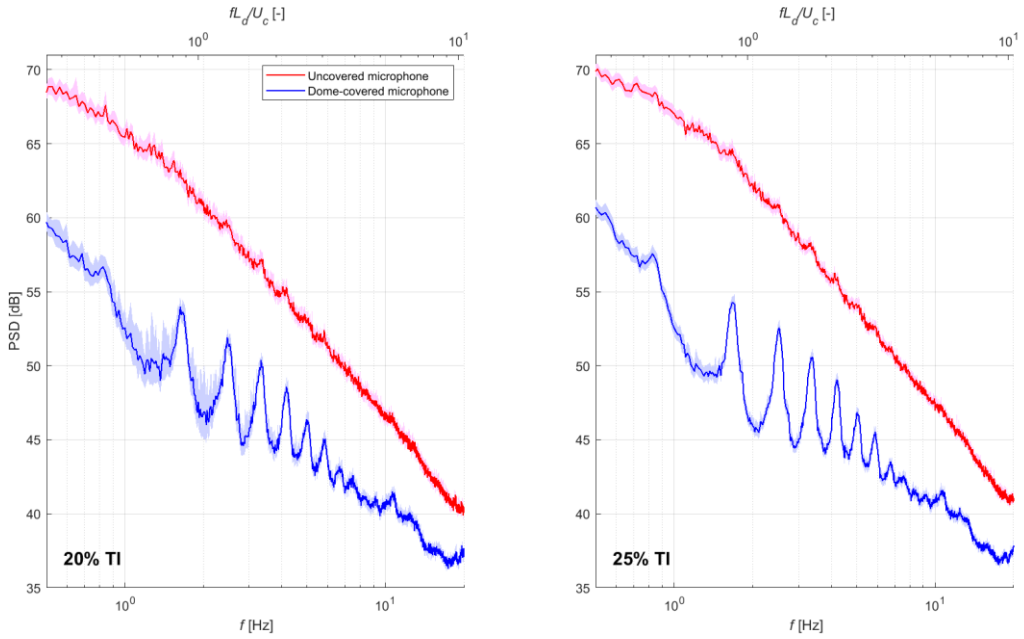

Fig. 10. (Absolute) PSD spectra for the uncovered and dome-covered microphone for 6 m/s mean wind speed and 20 and 25 % turbulence intensity in function of sound frequency (lower horizontal axis) and characteristic-length ratio (upper horizontal axis). The 95 % confidence intervals are calculated with the bootstrapping method, assuming no specific statistical distribution of the data, and are depicted as shaded areas.

Higher mean wind speeds allow to observe the effect of the dome in increasing the SNR for characteristic-length ratio down to approximately 0.2. The effect of the dome remains significant also for very turbulent atmospheres. The dome acts consistently to the principle of spherical wind screens as described by van den Berg [4], for which a spherical wind screen is able to significantly reduce microphone wind-induced noise down to characteristic-length ratio 0.3, overcoming the limitation of open fences where reductions were reported to drop abruptly at characteristic-length ratio below 1 [7]. The dome thus not only reduces the mean wind speed but acts on the turbulent eddies as a pressure averaging device as well [11], mitigating the resulting pressure fluctuations at the microphone membrane. The effect is largest for turbulence length scales of the same order of magnitude as the characteristic length of the dome and larger.

The differences in PSD spectra from both microphones were also analyzed in function of wind condition. The PSD differences in the infrasonic frequency range are presented in Figure 11 in dB and normalized for the reference pressure of $2 \cdot 10^{-5}$ Pa for mean wind speeds of 2, 3, 5 and 6 m/s and for different TIs.

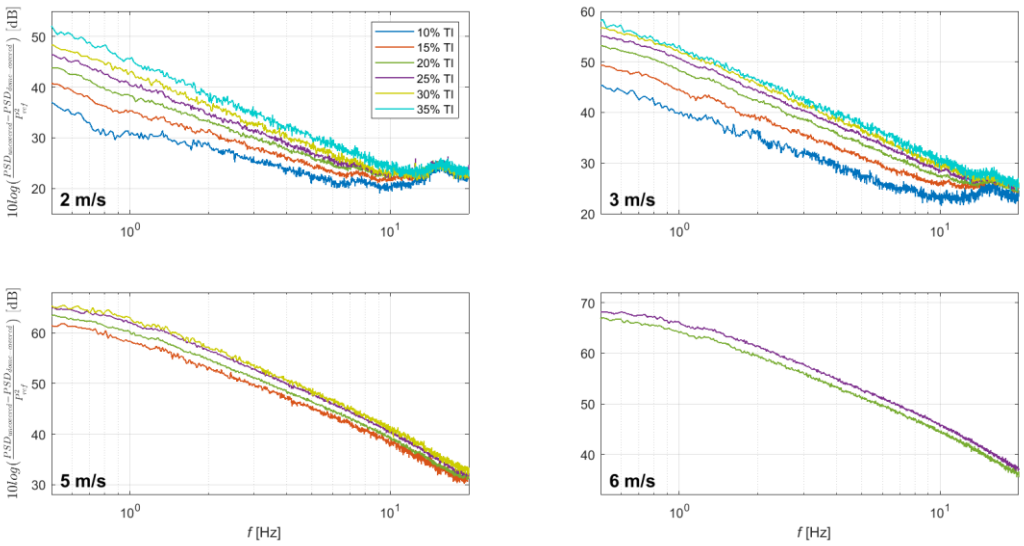

Fig. 11. Estimated mean wind-induced microphone noise at the uncovered microphone, calculated as normalized PSD spectra differences from the two microphone in dB for 2, 3, 5 and 6 m/s mean wind speed and different TIs.

At both microphones, PSD levels are the result of both wind-induced microphone noise and ambient noise. The wind-induced microphone noise will be different due to the action of the wind-shielding dome. The ambient noise, which includes also the wind turbines, remains the same for both microphones. Nevertheless, subtracting the PSD of the dome-covered microphone from the PSD of the uncovered microphone does not allow to determine the wind-induced noise reduction due to the dome as the contributions do not sum arithmetically. The noise sources are in fact coherent for the two microphones. The PSD difference provides an estimation of the noise level generated by the wind-induced microphone noise at the uncovered microphone.

Below 1 Hz, the estimated wind-induced microphone noise at 2 m/s mean wind speed is between 30 and 38 dB for 10 % TI and at 50 dB for 35 % TI. For all the mean wind speed cases, the estimated wind-induced microphone noise increases with increasing TI. Wind-induced

microphone noise depends on both mean wind speed and TI and it can reach 68 dB for 6 m/s mean wind speed and 25 % TI.

Moreover, the absolute levels at the uncovered microphone, as shown in Figures from 7 to 10, are comparable with the estimated wind-induced microphone noise level presented in Figure 11. Levels of the wind turbines, visible from the dome-covered microphone instead, are far below. The SNR at the uncovered microphone is thus poor while it is strongly increased by the presence of the dome for high mean wind speeds or high TIs.

4. Conclusions

A wind-shielding hemi-spherical dome for improving SNR for outdoor measurements of infrasound was designed and tested in detail. The shape of the structure and the porosity of the wind breaking textile were based on findings reported in literature and theoretical considerations regarding wind fence enclosures. The dome was shown to be nearly acoustically transparent in the low frequency range tested and within the limits of the experimental setup indoors. In an extensive outdoor test, the dome showed to reduce wind-induced microphone noise in the infrasonic spectral range down to a characteristic-length ratio of 0.2 or 0.5 Hz.

The wind-shielding dome allowed to clearly identify the tonal components in the infrasonic frequency range from wind turbines at close distance. At the non-dome covered microphone, these tones are mostly submersed in wind-induced microphone noise. Even at low mean wind speeds, the infrasonic wind-induced microphone noise at the non-dome covered microphone (but still with a standard 10-cm diameter spherical foam windscreen) shows to be strongly influenced by the turbulence intensity in the wind flow. The SNR is thus significantly improved by the dome, allowing to reveal the BPF and its harmonics, also at high TIs. Maximum improvement of the

SNR was seen for the case of 6 m/s mean wind speed at different TIs, occurring at approximately 1 Hz and a characteristic-length ratio 0.5.

The wind-shielding dome is thus a valid and advantageous apparatus for noise assessment of e.g. wind turbines, remaining compact in dimension. The dome allows a more accurate characterization of infrasonic emissions at higher mean wind speeds and/or stronger atmospheric turbulence degrees than would be possible with standard equipment.

Acknowledgements

This research is supported by the Special Research Fund (BOF 01J11015) from Ghent University. We are further grateful to the Biocentrum Agri-vet of Ghent University for allowing us to use their terrain while carrying out the field measurements. We also want to thank Vervaeke Bvba for tailoring their windbreak textile to our dome structure and Luminus for providing the operational data of the wind turbines.

References

[1] Morgan S, Raspet R. Investigation of the mechanisms of low-frequency wind noise generation outdoors. J Acoust Soc Am 1992;92:1180.

[2] Abbott J P, Raspet R, Webster J. Wind fence enclosures for infrasonic wind noise reduction. J Acoust Soc Am 2015;137:1265.

[3] Strasberg M. Dimensional analysis and windscreen noise. J Acoust Soc Am 1988;83:544.

[4] van Den Berg G P. Wind-induced noise in a screened microphone. J Acoust Soc Am 2005;119:824.

[5] Søndergaard B, Carsten R. Low Frequency Noise from Large Wind Turbines Sound Power Measurement Method. Copenhagen: Danish Energy Authority; 2008.

[6] Hansen K, Zajamsek B, Hansen C H. Identification of low frequency wind turbine noise using secondary wind screens of various geometries. Noise Control Engr J 2014;62:69.

[7] Hedlin M A H, Raspet R. Infrasonic wind-noise reduction by barrier and spatial filters. J Acoust Soc Am 2003;114(3):1379-86.

[8] Zajamzek B, Hansen K, Doola C J, Hansen C H. Characterization of wind farm infrasound and low-frequency noise. J Sound Vib 2016;370:176-190.

[9] Noble J M, Kirkpatrick W C A II, Raspet R, Collier S L, Coleman M A. Infrasonic wind noise reduction via porous fabric domes. In Proc of the 167th Meeting of the Acoustical Society of America, Providence; 2014.

[10] Abbott J P, Raspet R. Calculated wind noise for an infrasonic wind noise enclosure. J Acoust Soc Am. 2015;138:332.

[11] Raspet R, Abbott J P, Webster J, Yu J, Talmadge C, Kirkpatrick W C A II, Collier S L, Noble J M. New Systems for Wind Noise Reduction for Infrasonic Measurements, in *Infrasound*

Monitoring for Atmospheric Studies: Challenges in the Middle Atmospheric Dynamics and Societal Benefits 2nd edition, Springer 91-124.

[12] Collier S L, Raspet R, Noble J M, Kirkpatrick W C A II, Webster J, Abbott J P. Analysis of wind-noise reduction by semi-porous fabric domes. J Acoust Soc Am. 2014; 136(4):2139-2139.

[13] Dierickx W. Flow Reduction of Synthetic Screens Obtained with Both a Water and Airflow Apparatus. J Agr Eng Res 1998;71:67-73.